

Set-valued Young tableaux and product-coproduct prographs*

PAUL DRUBE

*Department of Mathematics and Statistics
Valparaiso University, Indiana, U.S.A.
paul.drube@valpo.edu*

MAXWELL KRUEGER

*Department of Mathematics and Computer Science
Muhlenberg College, Allentown, Pennsylvania, U.S.A.
mk250042@muhlenberg.edu*

ASHLEY SKALSKY

*Mathematics Department
Minnesota State University Moorhead, Minnesota, U.S.A.
borchardas@mnstate.edu*

MEGHAN WREN

*Department of Mathematics
SUNY Brockport, New York, U.S.A.
meghan.wren@daemen.edu*

Abstract

Standard set-valued Young tableaux are a generalization of standard Young tableaux where cells can contain unordered sets of integers, with the added condition that every integer at position (i, j) must be smaller than every integer at both $(i + 1, j)$ and $(i, j + 1)$. In this paper, we explore properties of standard set-valued Young tableaux with three rows and a fixed number of integers in every cell of each row. Our primary focus is on standard set-valued Young tableaux with 1 integer in each first-row cell, $k - 1$ integers in each second-row cell, and 1 integer in each third-row cell. For rectangular shapes $\lambda = n^3$, such tableaux are placed in bijection with closed k -ary product-coproduct prographs: directed plane

* Research supported by NSF Grant DMS-1559912.

graphs that correspond to finite compositions involving a k -ary product operator and a k -ary coproduct operator. That bijection is extended to three-row set-valued Young tableaux of non-rectangular and skew shape, and it is shown that a set-valued analogue of the Schützenberger involution corresponds to 180-degree rotation of the associated prographs. We also present direct enumerations of three-row standard set-valued Young tableaux with a fixed number of integers in every cell of each row.

1 Introduction

Consider a non-increasing sequence of positive integers $\lambda = (\lambda_1, \dots, \lambda_m)$ that sum to N . Following the English notation, a Young diagram Y of shape λ is a left-justified array of N cells with λ_i cells in the i^{th} row from the top of the array. Given a Young diagram of shape λ , a Young tableau of that shape is a bijection from the set of integers $[N] = \{1, \dots, N\}$ to the cells of Y . For a Young tableau to be a standard Young tableau, the entries in the tableau must increase left to right across each row and top to bottom down each column. We denote the set of standard Young tableaux of shape λ as $S(\lambda)$, and adopt the shorthand notation of $S(n^m)$ in the case of the m -row rectangular shape $\lambda = (n, \dots, n)$. For a thorough introduction to Young tableaux, see Fulton [7].

The number of standard Young tableaux of arbitrary shape λ may be directly calculated using the hook-length formula, as originally given by Frame, Robinson and Thrall [6]. A quick application of the hook-length formula to the case of $\lambda = (n, n)$ yields the well-known identity that $|S(n^2)| = C_n = \frac{(2n)!}{n!(n+1)!}$, the n^{th} Catalan number. Generalizing to the d -row rectangular case of $\lambda = (n, \dots, n)$ similarly yields $|S(n^d)| = C_{d,n}$, where $C_{d,n} = \frac{(d-1)!(dn)!}{n!(n+1)! \dots (n+d-1)!}$ is the n^{th} d -dimensional Catalan number.

Given a non-increasing sequence of positive integers $\lambda = (\lambda_1, \dots, \lambda_{m_1})$ that sum to N_1 and a non-increasing sequence of positive integers $\mu = (\mu_1, \dots, \mu_{m_2})$ that sum to N_2 , where $0 \leq \mu_i \leq \lambda_i$ for all i , one can define a skew Young diagram of shape λ/μ by removing the μ_i leftmost cells in the i^{th} row of the Young diagram of shape λ , for all $1 \leq i \leq m_2$. A skew Young tableau of shape λ/μ is a bijection from $[N_1 - N_2]$ to the cells of the skew Young diagram of shape λ/μ . Such a tableau is said to be a standard skew Young tableau if its entries increase left to right across each row and top to bottom down each column. We denote the set of standard skew Young tableaux of shape λ/μ by $S(\lambda/\mu)$.

This paper is focused on a generalization of standard Young tableaux known as standard set-valued Young tableaux. Consider a non-increasing sequence of positive integers $\lambda = (\lambda_1, \dots, \lambda_m)$ and a sequence of positive integers $\rho = (\rho_1, \dots, \rho_m)$ such that $\sum_{i=1}^m \lambda_i \rho_i = M$. A **set-valued Young tableau** of shape λ and (row-constant) **density** ρ is a function from $[M]$ to the cells of the Young diagram Y of shape λ such that every cell in the i^{th} row of Y receives precisely ρ_i integers. The resulting tableau qualifies as a **standard set-valued Young tableau** if, for each cell (i, j) of Y , every integer at position (i, j) is smaller than every integer in the cells at $(i+1, j)$ and $(i, j+1)$. In analogy with standard Young tableaux, we refer to these additional conditions

as “column-standardness” and “row-standardness”, respectively. We denote the set of standard set-valued Young tableaux of shape λ and density ρ as $\mathbb{S}(\lambda, \rho)$. See Figure 1 for a collection of standard set-valued Young tableaux with $\lambda = (3, 3) = 3^2$ and $\rho = (2, 1)$. Given a skew Young diagram of shape λ/μ , one may similarly define a **standard skew set-valued Young tableau** of shape λ/μ and (row-constant) density ρ . We denote the set of such skew tableaux by $\mathbb{S}(\lambda/\mu, \rho)$.

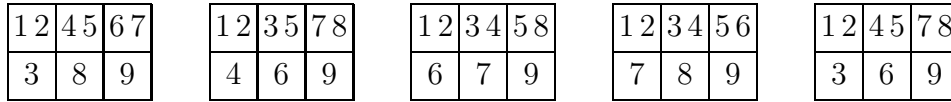


Figure 1: Five of the twelve elements of $\mathbb{S}(3^2, \rho)$ with $\rho = (2, 1)$.

Set-valued Young tableaux were originally introduced by Buch [3] to study the K -theory of Grassmannians. Heubach, Li and Mansour [8] later provided standard set-valued Young tableaux with $\lambda = n^2$ and row-constant density $\rho = (k - 1, 1)$ as one of their many combinatorial interpretations of the k -Catalan numbers $C_n^k = \frac{(kn)!}{(kn-n+1)!n!}$. That work was directly expanded upon by Drube [4], who used standard set-valued Young tableaux with two rows to provide new combinatorial interpretations of the Raney numbers, the rational Catalan numbers, and the solution to the generalized tennis ball problem. For recent usages of set-valued Young tableaux in a more algebraic setting, see Reiner, Tenner and Yong [11] and Monical [10].

It is important to emphasize the current lack of a set-valued analogue to the hook-length formula. This makes the enumeration of $\mathbb{S}(\lambda, \rho)$ for arbitrary λ and ρ an extremely challenging problem, and comprehensive attempts at counting standard set-valued Young tableaux of arbitrary density ρ have only been attempted for two-row shapes $\lambda = (a, b)$. See Drube [4] for calculations of $|\mathbb{S}(\lambda, \rho)|$ in the two-row rectangular case, enumerations that corresponded to various generalizations of the (two-dimensional) Catalan numbers.

With the two-row case relatively well-understood, this paper presents the first thorough investigation of standard set-valued Young tableaux in the case of three-row shapes. Much as various choices of ρ allow $|\mathbb{S}(n^2, \rho)|$ to correspond to various generalizations of the two-dimensional Catalan numbers, $|\mathbb{S}(n^3, \rho)|$ and certain choices of ρ will correspond to various generalizations of the three-dimensional Catalan numbers. To our knowledge, all three-dimensional Catalan generalizations discussed in this paper have yet to appear anywhere in the literature.

1.1 Outline of Paper

This paper proceeds as follows. In Section 2, we introduce k -ary product-coproduct prographs, a class of directed plane graphs that naturally extend existing combinatorial interpretations for both the two- and three-dimensional Catalan numbers. Much of Section 2 may be seen as an extension and formalization of the work of Borie [2]. This motivates our focus on the sets $\mathbb{S}(n^3, \rho)$ with $\rho = (1, k - 1, 1)$, which are placed in bijection with k -ary product-coproduct prographs (Theorem 2.1). In Section 3, we focus upon the enumeration of these tableaux, yielding a family of integers $C_{3,n}^k$.

that function as a three-dimensional analogue of the k -Catalan numbers. Closed formulas for $C_{3,n}^k$ are derived for $n \leq 5$ (Propositions 3.1, 3.2, 3.5, 3.6) and a general calculus is introduced to tackle the general case (Proposition 3.3). In Section 4, we further explore the bijection between our standard set-valued Young tableaux and k -ary product-coproduct prographs. Appropriately generalized prographs are placed in bijection with various sets of (non-rectangular and skew) standard set-valued Young tableaux (Theorem 4.2), and a 180-degree rotation of k -ary prographs is shown to correspond to a set-valued analogue of the Schützenberger involution on standard Young tableaux (Theorem 4.5). Section 5 closes the paper with a series of more cursory discussions, including a suggestion of additional combinatorial interpretations for $C_{d,n}^k$ and a consideration of three- and four-row set-valued tableaux with densities other than $\rho = (1, k - 1, 1)$.

2 k -ary Product-Coproduct Prographs and Set-Valued Tableaux

Let \mathcal{T}_n^k denote the set of full k -ary trees with $kn + 1$ vertices, drawn so that the root vertex lies at the bottom of the tree. It is well-known that \mathcal{T}_n^k is enumerated by the k -Catalan number $C_n^k = \frac{(kn)!}{(kn-n+1)!n!}$. In the $k = 2$ case, this prompts the well-studied bijection between \mathcal{T}_n^2 and $S(n^2)$ that associates entries in the top row of the tableau to left children and entries in the bottom row of the tableau to right children.

The bijection between \mathcal{T}_n^2 and $S(n^2)$ may be generalized to a bijection between \mathcal{T}_n^k and standard set-valued Young tableaux $\mathbb{S}(n^2, \rho)$ with row-constant density $\rho = (k - 1, 1)$. As described by Heubach, Li and Mansour [8], this generalized bijection $\phi_k : \mathcal{T}_n^k \rightarrow \mathbb{S}(n^2, \rho)$ is defined as below. For an example of ϕ_k , see Figure 2.

1. For any $T \in \mathcal{T}_n^k$, label the edges of T with the integers $\{1, \dots, nk\}$ according to a depth-left first search.
2. Place all integers that label rightmost-children of T in the bottom row of $\phi(T) \in \mathbb{S}(n^2, \rho)$, in increasing order from left to right.
3. Place all remaining integers from $\{1, \dots, nk\}$ in the top row of $\phi(T)$, in increasing order from left to right and ensuring that each cell in the top row receives precisely $k - 1$ integers.

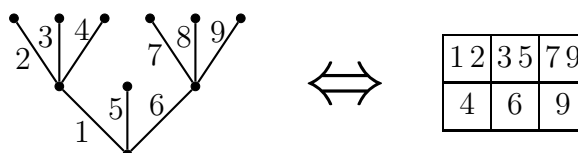


Figure 2: An example of the bijection $\phi_k : \mathcal{T}_n^k \rightarrow \mathbb{S}(n^2, \rho)$ for $k = 3$.

Following Borie [2], generalizing ϕ_k to three-row tableaux requires a consideration of prographs. For any finite collection G of formal operators, each of which is uniquely

identified by its number of inputs and outputs, one may consider the set of all finite compositions that are freely constructed using elements of G (as well as the identity operator Id). Each of these compositions corresponds to a directed planted plane graph in which all edges are directed upward. In these graphs, each application of a non-identity operator corresponds to a non-initial, non-terminal vertex whose vertical placement (when read from bottom to top) corresponds to the stage at which the operator appears in the composition. See Figure 3 for a quick example. Two planted plane graphs, drawn so that all edges maintain a strict upwards orientation, are considered equivalent if they represent equivalent formal operators. The resulting equivalence classes of such graphs constitute a set PRO_G that we refer to as the (free) prographs generated by G .

Let A denote a formal module. If G consists solely of an operator $\Delta_k : A \rightarrow A \otimes \cdots \otimes A$ with 1 input and k outputs (a non-coassociative k -ary coproduct), elements of PRO_G are a directed variation of full k -ary trees where every edge has been directed upward and a single input edge has been added below the root vertex. The subset of these prographs with precisely n usages of Δ_k are in bijection \mathcal{T}_n^k . For example, the 3-ary tree on the left side of Figure 2 corresponds the prograph shown in Figure 3.

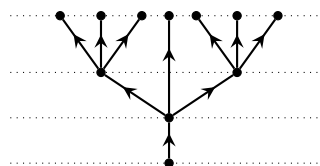


Figure 3: The prograph corresponding to the composition $(\Delta_3 \otimes \text{Id} \otimes \Delta_3) \circ \Delta_3$, where Δ_3 is a 3-ary coproduct.

Now consider the case where G consists of a (non-coassociative) k -ary coproduct $\Delta_k : A \rightarrow A \otimes \cdots \otimes A$ with 1 input and k outputs, as well as a (non-associative) k -ary product $\mu_k : A \otimes \cdots \otimes A \rightarrow A$ with k inputs and 1 output. We refer to the resulting elements of PRO_G as **k-ary (product-coproduct) prographs**. The subset of these prographs that have a single terminal vertex are known as **closed k-ary (product-coproduct) prographs**. As all prographs have a single initial vertex, all closed k -ary prographs must feature the same number of product and coproduct nodes. We denote the set of all closed k -ary prographs with precisely n products and n product by $\text{PC}^k(n)$. See Figure 4 for an illustration of $\text{PC}^2(2)$.

Borie [2] argued that $\text{PC}^2(n)$ is enumerated by the three-dimensional Catalan number $C_{3,n} = \frac{2(3n)!}{n!(n+1)!(n+2)!}$. This is accomplished by placing $\text{PC}^2(n)$ in bijection with the three-row standard Young tableaux $S(n^3)$.

Our goal for the rest of this section is to generalize Borie’s bijection to $\text{PC}^k(n)$ for all $k \geq 2$, where the appropriate k -generalization of $S(n^3)$ is standard set-valued Young tableaux $\mathbb{S}(n^3, \rho)$ with row-constant density $\rho = (1, k - 1, 1)$. We begin by introducing an algorithm for labelling the edges of any $G \in \text{PC}^k(n)$ that generalizes both the depth-left first labelling of k -ary trees and Borie’s depth-left search for elements of $\text{PC}^2(n)$.

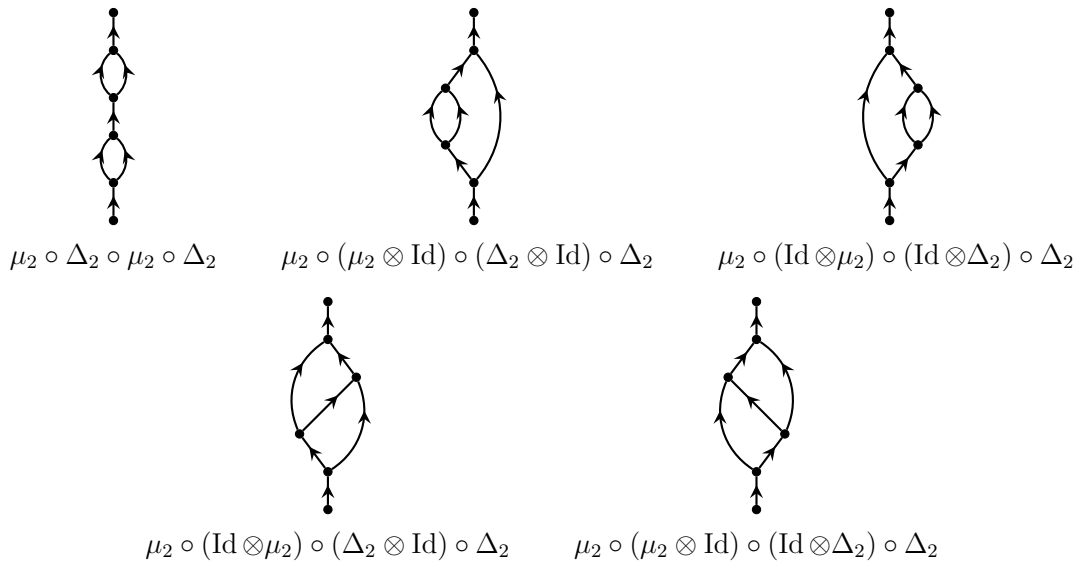


Figure 4: The set $\text{PC}^2(2)$ of closed 2-ary prographs with 2 products and 2 coproducts, atop a representative from the equivalence class to which each prograph corresponds.

1. Take any $G \in \text{PC}^k(n)$, and begin by labelling the sole output of the initial node of G with the integer 0.
2. For each $0 \leq i < nk$, recursively define a subgraph G_i of G consisting solely of edges labelled by $\{1, \dots, i\}$. Then let V_i denote the subset of nodes from G such that every input to that node lies in G_i and at least one output from that node lies in $G - G_i$.
3. Identify the highest labelled edge from G_i that terminates at an element v of V_i (this needn't be the edge labelled i). Then label the leftmost unlabelled edge of that vertex v with $i + 1$ and return to Step #2.

See Figure 5 for an example of this procedure, which we henceforth refer to as our (generalized) depth-left first search. Colloquially, the procedure may be described as “staying as leftward as possible, with the restriction that all inputs to a node must be labelled before any output from that node may be labelled”. Also notice that this procedure directly generalizes to non-closed k -ary prographs: one merely needs to omit terminal nodes from the V_i and repeat the recursive part of the algorithm until all terminal edges are labelled.

We are now ready to place $\text{PC}^k(n)$ in bijection with an appropriate collection of standard set-valued Young tableaux. Observe that Theorem 2.1 directly recovers the result of Borie [2] in the case of $k = 2$.

Theorem 2.1. *Fix $n \geq 1$ and $k \geq 2$. Then $|\text{PC}^k(n)| = |\mathbb{S}(n^3, \rho)|$ for $\lambda = n^3$ and $\rho = (1, k - 1, 1)$.*

Proof. We provide a pair of well-defined functions $\Phi : \text{PC}^k(n) \rightarrow \mathbb{S}(n^3, \rho)$, $\Phi_2 : \mathbb{S}(n^3, \rho) \rightarrow \text{PC}^k(n)$ and then show that $\Phi_2 = \Phi^{-1}$. Our first map $\Phi : \text{PC}^k(n) \rightarrow \mathbb{S}(n^3, \rho)$ is defined as below. See Figure 6 for an example.

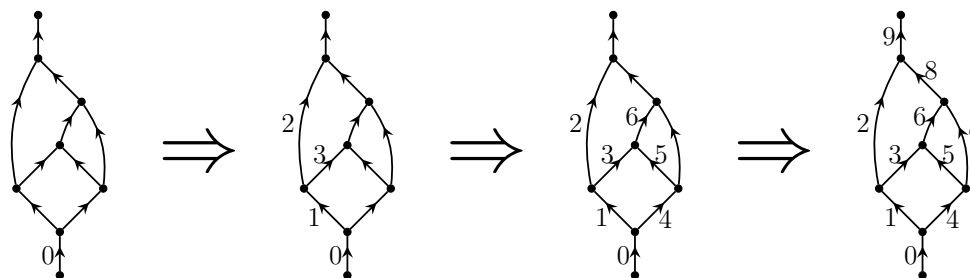


Figure 5: The generalized depth-left first search, applied to an element of $PC^2(3)$.

1. For any $G \in PC^k(n)$, label the edges of G via our depth-left first search.
2. Place integers that label leftmost coproduct children of G in the top row of $\Phi(G) \in \mathbb{S}(n^3, \rho)$, in increasing order from left to right.
3. Place integers that label all remaining coproduct children of G along the middle row of $\Phi(G)$, in increasing order from left to right and ensuring that each cell in the middle row receives precisely $k - 1$ integers.
4. Place integers corresponding to product children of G along the bottom row of $\Phi(G)$, in increasing order from left to right.

Notice that the initial input label of 0 is ignored in this procedure. As $\Phi(G)$ is row-standard by construction, to show that Φ is a well-defined map into $\mathbb{S}(n^3, \rho)$ we merely need to argue that $\Phi(G)$ is column-standard. Begin by noticing that our depth-left first search ensures that the leftmost child of a given coproduct node will always be labelled prior to the $k - 1$ non-leftmost children of that same node. This implies that every entry in the middle row of $\Phi(G)$ must be larger than the entry in the top row of the same column.

Now assume that precisely α_1 leftmost coproduct children and α_2 other coproduct children have been labelled prior to the labelling of the j^{th} product child of G . In order for the j^{th} product child to receive the next label, there must have been at least k previously labelled edges terminating at a node with an unlabelled output. Among the $\alpha_1 + \alpha_2 + (j - 1) + 1$ edges that were labelled prior to the labelling of the j^{th} product child (initial 0 edge included), precisely k edges terminate at each of the $j - 1$ product nodes with a previously labelled output, while 1 edge terminates at each of the α_1 coproduct nodes with a previously labelled leftmost output. This leaves $\alpha_1 + \alpha_2 + (j - 1) + 1 - k(j - 1) - \alpha_1 = \alpha_2 - (k - 1)j + k$ labelled edges that could lead into a product node with an unlabelled output. Enforcing $\alpha_2 - (k - 1)j + k \geq k$ gives $\alpha_2 \geq (k - 1)j$, ensuring that all entries in the middle row of the j^{th} column are smaller than the entry in the bottom row of the j^{th} column. It follows that $\Phi(G)$ is in fact column-standard and hence that Φ is well-defined.

For our second map $\Phi_2 : \mathbb{S}(n^3, \rho) \rightarrow PC^k(n)$, we recursively “build up” an edge-labelled prograph by working through $T \in \mathbb{S}(n^3, \rho)$ one entry at a time, as below.

1. For any $T \in \mathbb{S}(n^3, \rho)$, begin by placing an initial input edge labelled 0. Then recursively consider each entry $1 \leq i \leq (k + 1)n$ in numerical order.

2. If i lies in the top row of T , place a coproduct node whose input is the edge labelled $i - 1$. Then label the leftmost child of that coproduct with i .
3. If i is in the middle row of T , follow the depth-left first search through the partially constructed graph from the edge labelled $i - 1$. Then label the first unlabelled edge you encounter with the integer i .
4. If i is in the bottom row of T , place a product node whose rightmost input is the edge labelled $i - 1$ and whose remaining inputs are the $k - 1$ nearest terminal edges immediately to the left of the edge labelled $i - 1$. Then label the output of that product i .

The well-definedness of Φ_2 depends upon whether the actions described above are possible at every step. In particular, there must exist a rightward unlabelled edge when applying Step #3, and there must be enough leftward free edges (all previously labelled) when adding the product node in Step #4.

Begin by noting that, in the procedure that constructs $\Phi_2(T)$, leftmost coproduct children and product children are labelled as soon as they are placed. This means that unlabelled terminal edges at any intermediate step must correspond to non-leftmost coproduct children, and hence that all edges labelled in Step #3 must be non-leftmost coproduct children. Also notice that the edge labelled i immediately serves as an input for a new product or coproduct node unless $i + 1$ lies in the middle row of T . As this case involves an application of the depth-left first search, when initially placed $i + 1$ is always the rightmost terminal edge in our partially constructed prograph.

So assume that the entry i lies in the cell $(2, j)$ of T , and that i is larger than precisely x other integers in that cell ($0 \leq x \leq k - 2$). Row- and column-standardness of T guarantees that at least j coproducts have already been placed prior to this step, and that $(k - 1)(j - 1) + x$ of the non-leftmost children from those coproducts have already been labelled. This means there are at least $(k - 1)j - (k - 1)(j - 1) - x = k - 1 - x \geq 1$ unlabelled non-leftmost coproduct children at this step. Because all non-leftmost coproduct children are labelled according to our depth-left first search, all of these unlabelled coproduct edges lie to the left of the edge labelled $i - 1$. Thus the operation of Step #3 is always possible.

Now assume that i lies in the cell $(3, j)$ of T . Row- and column-standardness of T guarantee that at least j coproducts and precisely $j - 1$ products have already been placed at this point in the procedure, with at least kj coproduct children and precisely $j - 1$ product children having been labelled. As $j - 1$ labelled inputs are needed for the placement of each coproduct, this means that there are at least $kj - (k - 1)(j - 1) - (j - 1) = k$ labelled free edges when i is the active integer. Via preceding comments, the edge labelled $i - 1$ is the rightmost of these free edges. Thus the operation of Step #4 is always possible, and we may conclude that Φ_2 is well-defined.

It is only left to show that $\Phi_2 = \Phi^{-1}$. We demonstrate that $\Phi_2 \circ \Phi(G) = G$ for any $G \in PC^k(n)$, and that $\Phi \circ \Phi_2(T)$ for any $T \in \mathbb{S}(n^3, \rho)$.

To show $\Phi_2 \circ \Phi(G) = G$ for any $G \in \text{PC}^k(n)$, we inductively work through the edges of G in the order of the depth-left first search. For $i = 0$, G and $\Phi_2 \circ \Phi(G)$ both feature a single input edge labelled with i . For any $1 \leq i \leq n(k + 1)$, assume that G and $\Phi_2 \circ \Phi(G)$ feature identical sub-prographs (not necessarily closed) corresponding to the edges labelled $\{0, \dots, i - 1\}$. There are the three possible scenarios for the edge labelled i .

1. If $i - 1$ labels the input to a coproduct node in G , the edge labelled i must be the leftmost output of that same coproduct. This implies that i lies in the top row of $\Phi(G)$ and hence that $\Phi_2 \circ \Phi(G)$ also features a coproduct with input $i - 1$ and leftmost output i .
2. If $i - 1$ labels a non-rightmost input to a product node in G , the edge labelled i in G is always the next (on the right) input to that same product. That means that i lies in the middle row of $\Phi(G)$ and that the edge labelled with i in $\Phi_2 \circ \Phi(G)$ is determined via a depth-left first search from the edge labelled $i - 1$. This results in the next (on the right) input to that same product being labelled i in $\Phi_2 \circ \Phi(G)$.
3. If $i - 1$ labels the rightmost input to a product node in G , the edge labelled i in G is necessarily the output of that product. This implies that i lies in the bottom row of $\Phi(G)$ and thus that i also labels a product output in $\Phi_2 \circ \Phi(G)$ whose rightmost input is labelled $i - 1$.

As all three options lead to an identical placement of the edge labelled with i , we conclude $\Phi_2 \circ \Phi(G) = G$.

To show that $\Phi \circ \Phi_2(T) = T$ for any $T \in \mathbb{S}(n^3, \rho)$, we inductively work through the entries of T . For $i = 1$, T and $\Phi \circ \Phi_2(T)$ both feature i in the top-left corner. For $2 \leq i \leq n(k + 1)$, assume that T and $\Phi \circ \Phi_2(T)$ feature identical subtableau corresponding to the entries $\{1, \dots, i - 1\}$. There are again three possibilities for i :

1. If i lies in the top row of T , i labels a leftmost child of a coproduct node in $\Phi_2(T)$ whose input is labelled $i - 1$. Thus i lies in the top row of $\Phi \circ \Phi_2(T)$.
2. If i lies in the middle row of T , via earlier comments we know that i will always label a non-leftmost coproduct child in $\Phi_2(T)$. It follows that i also lies in the middle row of $\Phi \circ \Phi_2(T)$.
3. If i lies in the bottom row of T , i labels a product output in $\Phi_2(T)$ and hence i also lies in the bottom row of $\Phi \circ \Phi_2(T)$.

As all three cases lead to identical placement of i in the relevant tableaux, we conclude $\Phi \circ \Phi_2(T) = T$. □

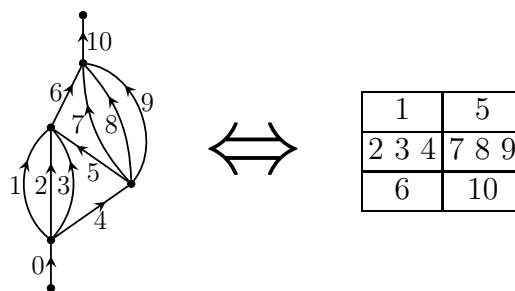


Figure 6: An example of the bijection $\Phi : \text{PC}^k(n) \rightarrow \mathbb{S}(n^3, \rho)$ for $n = 2$ and $k = 4$.

3 Enumerating $\mathbb{S}(n^3, \rho)$ for $\rho = (1, k - 1, 1)$

Theorem 2.1 suggests that $\mathbb{S}(n^3, \rho)$ with $\rho = (1, k - 1, 1)$ generalizes $S(n^3)$ in a manner similar to how $\mathbb{S}(n^2, \rho')$ with $\rho' = (k - 1, 1)$ generalizes $S(n^2)$. As the $\mathbb{S}(n^2, \rho')$ are enumerated by the k -Catalan numbers C_n^k , we henceforth refer to the cardinalities $|\mathbb{S}(n^3, \rho)| = C_{3,n}^k$ as the **three-dimensional k -Catalan numbers**.

The purpose of this section is to develop closed formulas for $C_{3,n}^k$. Sadly, developing such a formula or deriving a multivariate generating function for arbitrary $n \geq 1$, $k \geq 1$ do not appear to be tractable problems. As such, we restrict our attention to cases of small n . See Table 1 of Appendix 5.3 for a table of known values of $C_{3,n}^k$, which combines the explicit results of this section with calculations performed in Java.

In all that follows, notice that the “degenerate” $k = 1$ case corresponds to three-row tableaux with empty cells across their middle row. This means that the $k = 1$ enumerations reduce to pre-existing results about two-row tableaux: that $C_{3,n}^1 = |\mathbb{S}(n^3, \rho)| = |S(n^2)| = C_n$ for all $n \geq 1$ with $\rho = (1, 0, 1)$.

For all of our enumerations we recursively place $\mathbb{S}(\lambda, \rho)$ in bijection with a collection of sets $\bigcup \mathbb{S}(\lambda_i, \rho)$ of strictly smaller shape yet equivalent density. Our technique is similar to pre-existing proofs for non-set-valued tableaux where the sub-shapes λ_i are determined via the removal of lower-right corners, corresponding to possible locations of the largest possible entry in a tableau of shape λ . The difference here is that we never remove entries from a cell without eliminating all entries in that cell. If the removed cell contains entries other than the largest entry in the tableau, this necessitates that we account for the ordering of those smaller entries relative to integers appearing elsewhere in the tableau.

Before proceeding, note that $|S(\lambda, \rho)|$ is easily calculable when $\lambda = (n, 1, \dots, 1)$ is “hook-shaped”. In this case, one merely needs to count the ways of partitioning entries between the rightward and downward “legs”, giving an enumeration in terms of a single binomial coefficient $|S(\lambda, \rho)| = \binom{a}{b}$. See Figure 7 for examples.

For the rest of this section, an unfilled Young diagram of shape λ is used to denote the cardinality $|\mathbb{S}(\lambda, \rho)|$, assuming $\rho = (1, k - 1, 1)$.

Proposition 3.1. *Let $\rho = (1, k - 1, 1)$. For any $k \geq 1$, $C_{3,2}^k = |\mathbb{S}(2^3, \rho)| = k^2 + 1$.*

Proof. As the largest entry of any $T \in \mathbb{S}(2^3, \rho)$ must lie at $(3, 2)$, we investigate the integers $a_1 < \dots < a_{k-1}$ lying at $(2, 2)$ in an arbitrary set-valued tableaux

$$\begin{array}{|c|c|} \hline \square & \square \\ \hline \square & \\ \hline \square & \\ \hline \end{array} = \binom{k+1}{1} \qquad \begin{array}{|c|c|c|c|} \hline \square & \square & \square & \square \\ \hline \square & & & \\ \hline \square & & & \\ \hline \end{array} = \binom{k+3}{3}$$

Figure 7: Cardinalities $|S(\lambda, \rho)|$ for $\rho = (1, k - 1, 1)$ and a pair of hook-shapes λ . As 1 must lie at position $(1, 1)$, one merely needs to determine which of $\{2, 3, \dots\}$ lie in the remaining cells of the top row.

$T_1 \in \mathbb{S}(\lambda_1, \rho)$ of shape $\lambda_1 = (2, 2, 1)$. The only other entry in T_1 that may be larger than any of the a_i is the entry b at position $(3, 1)$. The subset of $\mathbb{S}(\lambda_1, \rho)$ satisfying $b \leq a_i$ for all i is then in bijection with $\mathbb{S}(\lambda_2, \rho)$ for $\lambda_2 = (2, 1, 1)$. If $b > a_1$, one must specify the ordering of b relative to a_2, \dots, a_{k-1} . So assume that j is the largest index such that $a_j < b$ (where $1 \leq j \leq k - 1$). Each choice of j defines a subset of $\mathbb{S}(\lambda_2, \rho)$ that is in bijection with $\mathbb{S}(\lambda_3, \rho)$ for $\lambda_3 = (2, 1)$, since for any choice of j the k largest entries of such a tableau $T_1 \in \mathbb{S}(\lambda_1, \rho)$ is split between positions $(2, 2)$ and $(3, 1)$. Combining these observations gives the string of equalities below.

$$\begin{array}{|c|c|} \hline \square & \square \\ \hline \square & \square \\ \hline \square & \square \\ \hline \end{array} = \begin{array}{|c|c|} \hline \square & \square \\ \hline \square & \square \\ \hline \square & \\ \hline \end{array} = \begin{array}{|c|c|} \hline \square & \square \\ \hline \square & \\ \hline \square & \\ \hline \end{array} + (k-1) \begin{array}{|c|c|} \hline \square & \square \\ \hline \square & \\ \hline \square & \\ \hline \end{array} = \binom{k+1}{1} + (k-1) \binom{k}{1} = k^2 + 1$$

□

Proposition 3.2. *Let $\rho = (1, k - 1, 1)$. For any $k \geq 1$,*

$$C_{3,3}^k = |\mathbb{S}(3^3, \rho)| = \frac{9k^4 - 2k^3 + 9k^2}{4} + 1.$$

Proof. We begin by enumerating $\mathbb{S}(\lambda', \rho)$ for $\lambda' = (3, 2, 1)$. For arbitrary $T' \in \mathbb{S}(\lambda', \rho)$, let $a_1 < \dots < a_{k-1}$ denote the entries at $(2, 2)$, b denote the entry at $(3, 1)$, and c denote the entry at $(1, 3)$. Proceeding as in the proof of Proposition 3.1, we subdivide $\mathbb{S}(\lambda', \rho)$ based on the relationship of b and c to the a_i and then delete all entries $x \geq a_1$ to place each subset in bijection with tableaux of some smaller shape. The equalities below summarize our results, with the first summand corresponding to $b, c < a_1$, the second summand corresponding to the $k - 1$ placements of b relative to $a_2 < \dots < a_{k-1}$ when $b > a_1$ yet $c < a_1$, the third summand corresponding to the $k - 1$ placements of c relative to $a_2 < \dots < a_{k-1}$ when $c > a_1$ yet $b < a_1$, and the fourth summand corresponding to the $\binom{k}{k-2, 1, 1}$ placements of b, c relative to $a_2 < \dots < a_{k-1}$ when $b, c > a_1$.

$$\begin{array}{|c|c|c|} \hline \square & \square & \square \\ \hline \square & \square & \\ \hline \square & & \\ \hline \end{array} = \begin{array}{|c|c|c|} \hline \square & \square & \square \\ \hline \square & & \\ \hline \square & & \\ \hline \end{array} + \binom{k-1}{1} \begin{array}{|c|c|c|} \hline \square & \square & \square \\ \hline \square & & \\ \hline \square & & \\ \hline \end{array} + \binom{k-1}{1} \begin{array}{|c|c|} \hline \square & \square \\ \hline \square & \\ \hline \square & \\ \hline \end{array} + \binom{k}{k-2, 1, 1} \begin{array}{|c|c|} \hline \square & \square \\ \hline \square & \\ \hline \square & \\ \hline \end{array} =$$

$$\binom{k+2}{2} + \binom{k-1}{1} \binom{k+1}{2} + \binom{k-1}{1} \binom{k+1}{1} + \binom{k}{k-2, 1, 1} \binom{k}{1} = \frac{3k^3 + k^2 + 2k}{2}.$$

For the full theorem, we once again proceed as in the proof to Proposition 3.1. After reducing to arbitrary $T \in \mathbb{S}(\lambda, \rho)$ with $\lambda = (3, 3, 2)$, we divide $\mathbb{S}(\lambda, \rho)$ into subsets depending upon how the entries $a_1 < \dots < a_{k-1}$ at position $(2, 3)$ relate to the entry b_1 at $(3, 1)$ and the entry b_2 at $(3, 2)$. The three summands in the first line of the equalities below corresponds to the cases of $b_1 < b_2 < a_1$, $b_1 < a_1 < b_2$, and $a_1 < b_1 < b_2$, respectively. In the second line of equalities, the first of those subsets is further subdivided based upon the relationship of the entry c at $(1, 3)$ to the entry b_2 at $(3, 2)$, with the two new summands corresponding to $b_2 < c$ and $c < b_2$, respectively. This leaves a sum of cardinalities $|\mathbb{S}(\lambda_i, \rho)|$ that are computable via Proposition 3.1, our informal lemma for shape $\lambda' = (3, 2, 1)$, and the result of Heubach, Li and Mansour [8] giving $|\mathbb{S}(n^2, \rho)| = C_n^k$.

$$\begin{aligned}
 \begin{array}{|c|c|c|} \hline \square & \square & \square \\ \hline \square & \square & \square \\ \hline \square & \square & \square \\ \hline \end{array} &= \begin{array}{|c|c|c|} \hline \square & \square & \square \\ \hline \square & \square & \square \\ \hline \square & \square & \square \\ \hline \end{array} = \begin{array}{|c|c|c|} \hline \square & \square & \square \\ \hline \square & \square & \square \\ \hline \square & \square & \square \\ \hline \end{array} + \binom{k-1}{1} \begin{array}{|c|c|c|} \hline \square & \square & \square \\ \hline \square & \square & \square \\ \hline \square & \square & \square \\ \hline \end{array} + \binom{k}{2} \begin{array}{|c|c|c|} \hline \square & \square & \square \\ \hline \square & \square & \square \\ \hline \square & \square & \square \\ \hline \end{array} \\
 &= \begin{array}{|c|c|c|} \hline \square & \square & \square \\ \hline \square & \square & \square \\ \hline \square & \square & \square \\ \hline \end{array} + \begin{array}{|c|c|c|} \hline \square & \square & \square \\ \hline \square & \square & \square \\ \hline \square & \square & \square \\ \hline \end{array} + \binom{k-1}{1} \begin{array}{|c|c|c|} \hline \square & \square & \square \\ \hline \square & \square & \square \\ \hline \square & \square & \square \\ \hline \end{array} + \binom{k}{2} \begin{array}{|c|c|c|} \hline \square & \square & \square \\ \hline \square & \square & \square \\ \hline \square & \square & \square \\ \hline \end{array} \\
 &= (k^2 + 1) + k \left(\frac{3k^3 + k^2 + 2k}{2} \right) + \binom{k}{2} C_3^k = \frac{9k^4 - 2k^3 + 9k^2}{4} + 1
 \end{aligned}$$

□

The proofs of Propositions 3.1 and 3.2 suggest a general methodology for enumerating $\mathbb{S}(n^3, \rho)$ that could be applied to all $n \geq 2$. In particular, for any three-row shape our technique of removing every entry in a lower-right corner yields the recurrences of Proposition 3.3.

Proposition 3.3. *Fix $k \geq 1$. For $\rho = (1, k - 1, 1)$ and any three-row shape $\lambda = (a, b, c)$ with $a \leq b \leq c$,*

$$|\mathbb{S}((a, b, c), \rho)| = \begin{cases} \sum_{\substack{0 \leq i \leq a-b, \\ 0 \leq j \leq c}} \binom{k-2+i+j}{k-2, i, j} |\mathbb{S}((a-i, b-1, c-j), \rho)|, & \text{if } b > c; \\ \sum_{0 \leq i \leq a-b} |\mathbb{S}((a-i, b, c-1), \rho)|, & \text{if } b = c. \end{cases}$$

Notice that, although we have utilized other results about hook-shaped tableaux and two-row tableaux to shorten our proofs in the $n = 2, 3$ cases, the two recurrences of Proposition 3.3 are sufficient to reduce any $|\mathbb{S}((a, b, c), \rho)|$ to a summation involving one-column shapes λ_i , where $|\mathbb{S}(\lambda_i, \rho)| = 1$. Considered as a function of k , we may then use Proposition 3.3 to quickly draw several conclusions about $|\mathbb{S}((a, b, c), \rho)|$:

Corollary 3.4. Fix $\rho = (1, k - 1, 1)$, where k is indeterminate, and let $\lambda = (a, b, c)$ satisfy both $b \geq 1$ and $a + c \geq 2$. If $a = b = c$, then $|\mathbb{S}((a, b, c), \rho)|$ is a polynomial in k of degree $a + c - 2$. If $a > c$, then $|\mathbb{S}((a, b, c), \rho)|$ is a polynomial in k of degree $a + c - 1$.

Proof. That $|\mathbb{S}((a, b, c), \rho)| = p(k)$ is a polynomial in k follows directly from the recursion of Proposition 3.4. To demonstrate the degree of $p(k)$, induct on $i = a + b + c$ for $i \geq 3$. The base case of $i = 3$ follows from $|\mathbb{S}((2, 1, 0), \rho)| = k$ and $|\mathbb{S}((1, 1, 1), \rho)| = 1$. For the inductive case, take $|\mathbb{S}((a, b, c), \rho)|$ with $a + b + c = i + 1$. If $b > c$, the first case of Proposition 3.4 equates $|\mathbb{S}((a, b, c), \rho)|$ with a sum of polynomials (all with positive leading coefficient) whose maximal degree summand(s) all have degree $a + c - 1$. If $b = c$, the second case of Proposition 3.4 equates $|\mathbb{S}((a, b, c), \rho)|$ with a sum of polynomials whose sole maximal degree summand has degree $a + (c - 1) - 1$. \square

In the case of $\lambda = n^3$, notice that Corollary 3.4 implies that $p(k) = |\mathbb{S}(n^3, \rho)|$ has degree $2(n - 1)$. Proposition 3.3 may also be applied with the aid of a computer algebra system to derive the following polynomials, corresponding to $C_{3,4}^k$ and $C_{3,5}^k$.

Proposition 3.5. Let $\rho = (1, k - 1, 1)$. For any $k \geq 1$,

$$|\mathbb{S}(4^3, \rho)| = \frac{256k^6 - 114k^5 + 217k^4 - 12k^3 + 121k^2}{36} + 1.$$

Proposition 3.6. Let $\rho = (1, k - 1, 1)$. For any $k \geq 1$,

$$|\mathbb{S}(5^3, \rho)| = \frac{15625k^8 - 10092k^7 + 10258k^6 - 72k^5 + 5473k^4 - 204k^3 + 2628k^2}{576} + 1.$$

4 Properties of k -ary Prographs

In this section we prove a generalization of Theorem 2.1 that applies to non-closed k -ary prographs satisfying certain basic properties. We then explore one significant application of our bijection that generalizes an unproven proposition of Borie [2], showing that 180-degree rotation of prographs corresponds to a set-valued analogue of the Schützenberger involution on standard Young tableaux.

4.1 Non-Closed k -ary Prographs and Set-Valued Tableaux

We begin by generalizing the set PRO_G to finite compositions of formal operators where the initial input is the an x -fold tensor product $A \otimes \cdots \otimes A$ of the formal module A . The resulting directed plane graphs resemble prographs over G but now contain precisely x input strands, aligned horizontally across the bottom of the graph. Fixing G and $m \geq 1$, we may enforce a notion of equivalence on the resulting set of directed plane graphs that is analogous to the equivalence relation on PRO_G from Section 2. We refer to the resulting set of equivalence classes $\text{PRO}_{G,x}$ as the set of x -fold (free) prographs generated by G .

In the case where G consists of a k -ary coproduct Δ_k and a k -ary product μ_k , we refer to the elements of $\text{PRO}_{G,x}$ as **x -fold k -ary (product-coproduct) prographs**. We denote the subset of x -fold k -ary prographs with precisely n coproduct nodes and m product nodes by $\text{PC}_x^k(n, m)$. Notice that these three parameters are sufficient to determine the number of output strands in any $G \in \text{PC}_x^k(n, m)$. Explicitly,

Proposition 4.1. *Take any $G \in \text{PC}_x^k(n, m)$. Then G has precisely $y = (n - m)(k - 1) + x$ output strands. In particular, $y \equiv x \pmod{k - 1}$.*

Proof. Observe that each k -ary coproduct increases the number of free edges by $k - 1$, while each k -ary product decreases the number of free edges by $k - 1$. If we begin with x free edges, after n coproducts and m products we have $y = x + n(k - 1) - m(k - 1)$ outgoing free edges. \square

For any $x \equiv 1 \pmod{k - 1}$, consider $\text{PC}_x^k(n, m)$. There exists an injection $j : \text{PC}_x^k(n, m) \rightarrow \text{PC}^k(n + \frac{x-1}{k-1})$ that is defined by recursively joining incoming strands with k -ary coproducts, from left to right in sets of k , while recursively joining outgoing strands with k -ary products, from right to left in sets of k . See Figure 8 for an illustration. For any $G \in \text{PC}_x^k(n, m)$, we call the image $j(G) \in \text{PC}^k(n + \frac{x-1}{k-1})$ the **justification** of G . Assuming $x \equiv 1 \pmod{k - 1}$, justification suggests the generalization of Theorem 2.1 given by Theorem 4.2.

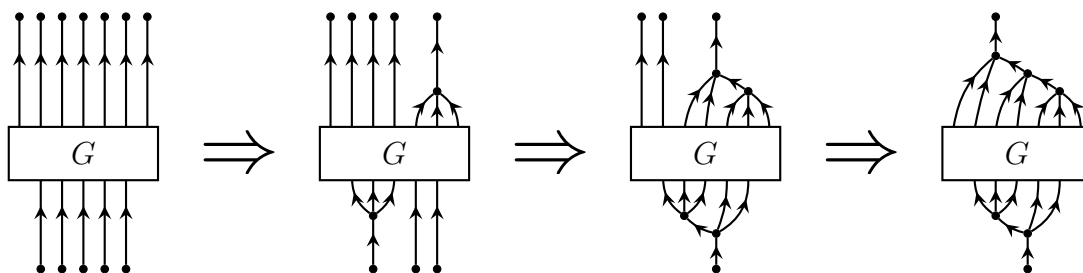


Figure 8: A non-closed prograph $G \in \text{PC}_5^3(n, n - 1)$ and its justification $j(G) \in \text{PC}^3(n + \frac{5-1}{3-1})$.

Theorem 4.2. *Fix $n, m \geq 1, k \geq 2$, and take any $x \geq 1$ such that $x \equiv 1 \pmod{k - 1}$. Then $|\text{PC}_x^k(n, m)| = |\mathbb{S}(\lambda/\mu, \rho)|$, where $\lambda = (n + \frac{x-1}{k-1}, n + \frac{x-1}{k-1}, m)$, $\mu = (\frac{x-1}{k-1}, 0, 0)$, and $\rho = (1, k - 1, 1)$.*

Proof. Let $j : \text{PC}_x^k(n, m) \rightarrow \text{PC}^k(n + \frac{x-1}{k-1})$ be justification and let $\Phi : \text{PC}^k(n + \frac{x-1}{k-1}) \rightarrow \mathbb{S}((n + \frac{x-1}{k-1})^3, \rho)$ be the forward bijection from Theorem 2.1. Then define $\chi : \mathbb{S}((n + \frac{x-1}{k-1})^3, \rho) \rightarrow \mathbb{S}(\lambda/\mu, \rho)$ as the map that deletes the first $\frac{x-1}{k-1}$ cells in the top row of $T \in \mathbb{S}((n + \frac{x-1}{k-1})^3, \rho)$, deletes the last $\frac{y-1}{k-1}$ cells in the bottom row of T , and then reindexes all remaining entries so that no positive integers are skipped. We define $\psi : \text{PC}_x^k(n, m) \rightarrow \mathbb{S}(\lambda/\mu, \rho)$ by $\psi = \chi \circ \Phi \circ j$, and show that ψ is a bijection. See Figure 9 for an example of this map ψ .

Well-definedness of j, Φ , and χ ensure that the composition ψ is also well-defined. To show that ψ is a bijection, we begin showing that the restriction $\tilde{\chi} = \chi|_{\text{im}(\Phi \circ j)}$

is a bijection onto $\mathbb{S}(\lambda/\mu, \rho)$. So take any $G \in \text{PC}_x^k(n, m)$. Using Proposition 4.1, the number of output strands in G is $y = (k - 1)(n - m) + x$. Thus $n + \frac{x-1}{k-1} = m + \frac{y-1}{k-1}$, and $j(G) \in \text{PC}^k(n + \frac{x-1}{k-1})$ is obtained from G by recursively adding $\frac{x-1}{k-1}$ left-aligned coproducts to the bottom of G and $\frac{y-1}{k-1}$ right-aligned products to the top of G . Applying our depth-left first search to $j(G)$ then results in the first $\frac{x-1}{k-1}$ non-zero labels being applied to the leftmost children of the “new” coproduct nodes at the bottom of $j(G)$, while the final $\frac{y-1}{k-1}$ labels are applied to the outputs of the “new” product nodes at the top of $j(G)$. This guarantees that the first row of every $T \in \text{im}(\phi \circ j)$ begins with $1, \dots, \frac{x-1}{k-1}$ and that the bottom row of every such T ends with $k(n + \frac{x-1}{k-1}) + m + 1, \dots, (k + 1)(n + \frac{x-1}{k-1})$. It follows that the entries deleted by χ are identical across all tableaux in $\tilde{\chi}$, implying that $\tilde{\chi}$ is a bijection.

Bijectivity of $\tilde{\chi}$ implies that $\chi \circ \Phi$ is also bijective with inverse $(\chi \circ \Phi)^{-1} \equiv \Phi^{-1} \circ \tilde{\chi}^{-1}$. Notice that $\tilde{\chi}^{-1} : \mathbb{S}(\lambda/\mu, \rho) \rightarrow \mathbb{S}((n + \frac{x-1}{k-1})^3, \rho)$ is the function that reindexes all entries of $T \in \mathbb{S}(\lambda/\mu, \rho)$ by $a \mapsto a + \frac{x-1}{k-1}$, appends $\{1, \dots, \frac{x-1}{k-1}\}$ to the front of the top row, and appends the $\frac{y-1}{k-1}$ entries $\{k(n + \frac{x-1}{k-1}) + m + 1, \dots, (k + 1)(n + \frac{x-1}{k-1})\}$ to the end of the bottom row. This means that $\text{im}(\Phi^{-1} \circ \tilde{\chi}^{-1})$ are the prographs $G \in \text{PC}^k(n + \frac{x-1}{k-1})$ with $\frac{x-1}{k-1}$ consecutive left-aligned coproducts at the bottom and $\frac{y-1}{k-1}$ consecutive right-aligned products at the top.

All of this allows us to define an “unjustification” map $h : \text{im}(\Phi^{-1} \circ \tilde{\chi}^{-1}) \rightarrow \mathbb{S}(\lambda/\mu, \rho)$ where, for any prograph $G \in \text{im}(\Phi^{-1} \circ \tilde{\chi}^{-1})$, one simply deletes the $\frac{x-1}{k-1}$ initial product nodes (along with their inputs) and deletes the $\frac{y-1}{k-1}$ final coproduct nodes (along with their outputs). This map h clearly satisfies $j \circ h(G) = G$ for any $G \in \text{im}(\Phi^{-1} \circ \tilde{\chi}^{-1})$ and $h \circ j(G) = G$ for any $G \in \mathbb{S}(\lambda/\mu, \rho)$. We may then conclude that ψ is a bijection with inverse $(\chi \circ \Phi \circ j)^{-1} \equiv h \circ \Phi^{-1} \circ \tilde{\chi}^{-1}$. \square

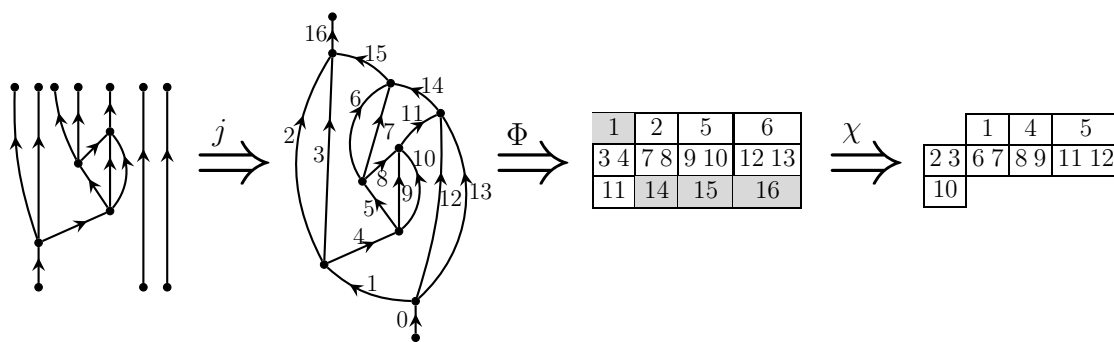


Figure 9: An example of the bijection $\psi : \text{PC}_x^k(n, m) \rightarrow \mathbb{S}(\lambda/\mu, \rho)$ for $k = 3$, $x = 3$, $n = 3$, and $m = 1$.

In light of Theorem 4.2, one may define a modification of our depth-left first search that allows one to pass directly from an edge-labelling of $G \in \text{PC}_x^k(n, m)$ to $\psi(G) \in \mathbb{S}(\lambda/\mu, \rho)$, bypassing the justification and reindexing steps. This x -fold depth-left first search is defined as below.

1. For any $G \in \text{PC}_x^k(n, m)$ with $x \equiv 1 \pmod{k - 1}$, label the leftmost initial input of G with the integer 0.

2. After labelling the i^{th} edge, determine the node subset V_i from the depth-left first search of Section 2. If V_i is non-empty, follow the procedure of Section 2 to find the edge labelled $i + 1$. If V_i is empty, label the leftmost unlabelled initial input of G with $i + 1$

Using the same terminology as Theorem 4.2, let $\tau(G) \in \mathbb{S}(\lambda/\mu, \rho)$ be the tableau that results from applying the x -fold depth-left first search to $G \in PC_x^k(n, m)$, placing all integers labelling leftmost coproduct children of G in the top row, placing all integers labelling product children of G in the bottom row, and placing all remaining non-zero integers (including those labelling non-leftmost initial inputs of G) in the middle row. This is in fact that same tableau that results from the composite bijection of Theorem 4.2:

Corollary 4.3. *Let $\psi : PC_x^k(n, m) \rightarrow \mathbb{S}(\lambda/\mu, \rho)$ be as in the proof of Theorem 4.2. For any $G \in PC_x^k(n, m)$ with $x \equiv 1 \pmod{k-1}$, $\tau(G) = \psi(G)$.*

Proof. Recall that justification of G introduces precisely $\frac{x-1}{k-1}$ leftmost coproduct children that receive the first $\frac{x-1}{k-1}$ nonzero labels in the depth-left first search on $j(G)$, as well as $\frac{y-1}{k-1}$ product children that receive the final $\frac{y-1}{k-1}$ labels in the depth-left first search on $j(G)$. As these are precisely the entries of $\Phi \circ j(G)$ that are deleted in the final stage of ψ , we merely need to argue that the depth-left first search of Section 2 labels the remaining edges of $j(G)$ in the same order that the x -fold depth-left first search labels the edges of G . In particular, we need to show that the i^{th} edge from the x -fold depth-left first search on G corresponds to the $(i + \frac{x-1}{k-1})^{th}$ edge from our original depth-left first search on $j(G)$.

Inducting on i , consider the two algorithms after the labelling of the i^{th} edge of G . If the set V_i is non-empty for G , the set $V_{(i+\frac{x-1}{k-1})}$ is non-empty for $j(G)$. Since the inputs to the initial coproduct nodes that appear only in $j(G)$ have lower edge labels than all other edges in $j(G)$, the element of V_i in G with the largest input corresponds to the element of $V_{(i+\frac{x-1}{k-1})}$ in $j(G)$ with the largest input. This leads to equivalent placements of the next edge label in both graphs. Now if V_i is empty for G , it must be the case that $V_{(i+\frac{x-1}{k-1})}$ for $j(G)$ consists solely of nodes from the justification’s $\frac{x-1}{k-1}$ initial coproducts. As the edge labels on the inputs to these initial coproducts always decrease from left to right, the next edge labelled in $j(G)$ is always the leftmost output of the initial coproducts that has yet to be labelled. These initial coproduct children of $j(G)$ precisely correspond to initial inputs in the non-justified graph G , implying that the next edge of G to be labelled by the x -fold depth-left first search is the equivalent (non-leftmost) initial input of G . □

4.2 The Schützenberger Involution

For any rectangular shape $\lambda \vdash N$, the Schützenberger involution is a map $f : S(\lambda) \rightarrow S(\lambda)$ that rotates $T \in S(\lambda)$ by 180 degrees and then rennumbers entries via $a \mapsto N - a + 1$. As described by Drube [4], one may define an analogue of the Schützenberger involution for standard set-valued Young tableaux. For any rectangular shape λ

and row-constant density ρ , the set-valued Schützenberger involution $f : \mathbb{S}(\lambda, \rho) \rightarrow \mathbb{S}(\lambda, \rho')$ is similarly defined via 180-degree rotation of $T \in \mathbb{S}(\lambda, \rho)$, followed by a reversal in the order of entries in the resulting tableaux. Here $\rho' = (\rho_m, \dots, \rho_1)$ if $\rho = (\rho_1, \dots, \rho_m)$, meaning only “vertically symmetric” densities are preserved by f .

Now define a rotation operator $r : \text{PC}_x^k(n, m) \rightarrow \text{PC}_y^k(m, n)$ on (not-necessarily closed) k -ary prographs that corresponds to 180-degree rotation and a reversal in the orientation of all edges. In Theorem 4.5 we will show that a specialization of this operator to any closed k -ary prograph G is compatible with the Schützenberger involution on the associated set-valued tableaux $\Phi(G)$ from Theorem 2.1, but first we need to analyze how rotation effects our edge-labelling algorithms. It is in fact that case that the x -fold depth-left first search of Subsection 4.1 labels the edges of $r(G) \in \text{PC}_y^k(m, n)$ in an order that exactly reverses the order in which it labels the corresponding edges of $G \in \text{PC}_x^k(n, m)$:

Proposition 4.4. *For any $k \geq 2$, $n, m \geq 0$, $x \geq 1$, set $N = x + kn + m - 1$ and consider the rotation operator $r : \text{PC}_x^k(n, m) \rightarrow \text{PC}_y^k(m, n)$. For any edge e of G , if the x -fold depth-left first search labels e with the integer i , then the x -fold depth-left first search labels the corresponding edge of $r(G)$ with $N - i$.*

Proof. We proceed by induction on the maximum edge label $N \geq 0$. The $N = 0$ case is immediate, as both G and $r(G)$ consist of a single edge labelled 0. For $N > 0$, consider the edge e of G that receives the label N , which is always the rightmost output of G . There are three options: 1) e is a “free strand” that does not originate at a product or coproduct, 2) e is a product child, or 3) e is a rightmost coproduct child.

If e is a free strand, simply deleting e produces a valid prograph \tilde{G} with maximal edge label $N - 1$. By the inductive hypothesis, the x -fold depth-left first search labels corresponding edges in \tilde{G} and $r(\tilde{G})$ according to $i \mapsto N - 1 - i$. Inserting a free strand (labelled 0) on the left side of G recovers $r(G)$, and effects our edge labelling in that the label of all edges in $r(\tilde{G})$ are increased by 1. It follows that the x -fold depth-left first search labels corresponding edges in G and $r(G)$ according to $i \mapsto N - i$.

If e is a product child, we eliminate the product node at the source of e as in the first row of Figure 10, yielding a prograph \tilde{G} with $k - 1$ additional outputs but maximal edge label $N - 1$. Applying the inductive hypothesis allows us to relate corresponding edge labels of \tilde{G} and $r(\tilde{G})$ by $i \mapsto N - 1 - i$. We then pre-compose $r(\tilde{G})$ with an additional coproduct whose outputs are the k leftmost inputs of $r(\tilde{G})$, as in the top row of Figure 10. This recovers $r(G)$ and effects our edge labelling in that all edges apart from the new coproduct input are increased by 1. It follows that the x -fold search labels corresponding edges in G and $r(G)$ according to $i \mapsto N - i$.

Lastly, if e is a rightmost coproduct child we eliminate the coproduct node at the source of e as in the bottom row of Figure 10, identifying the input of that coproduct with its leftmost output while extending all remaining outputs of to the bottom of the prograph as $k - 1$ new inputs. As the resulting graph \tilde{G} has maximal edge label $N - 1$, we may once again relate corresponding edge labels of \tilde{G} and $r(\tilde{G})$ by $i \mapsto N - 1 - i$. Introducing a new product node into $r(\tilde{G})$ as in the bottom

row of Figure 10 recovers $r(G)$ and effects our x -fold search in such a way that the corresponding edges of G and $r(G)$ are labelled according to $i \mapsto N - i$. \square

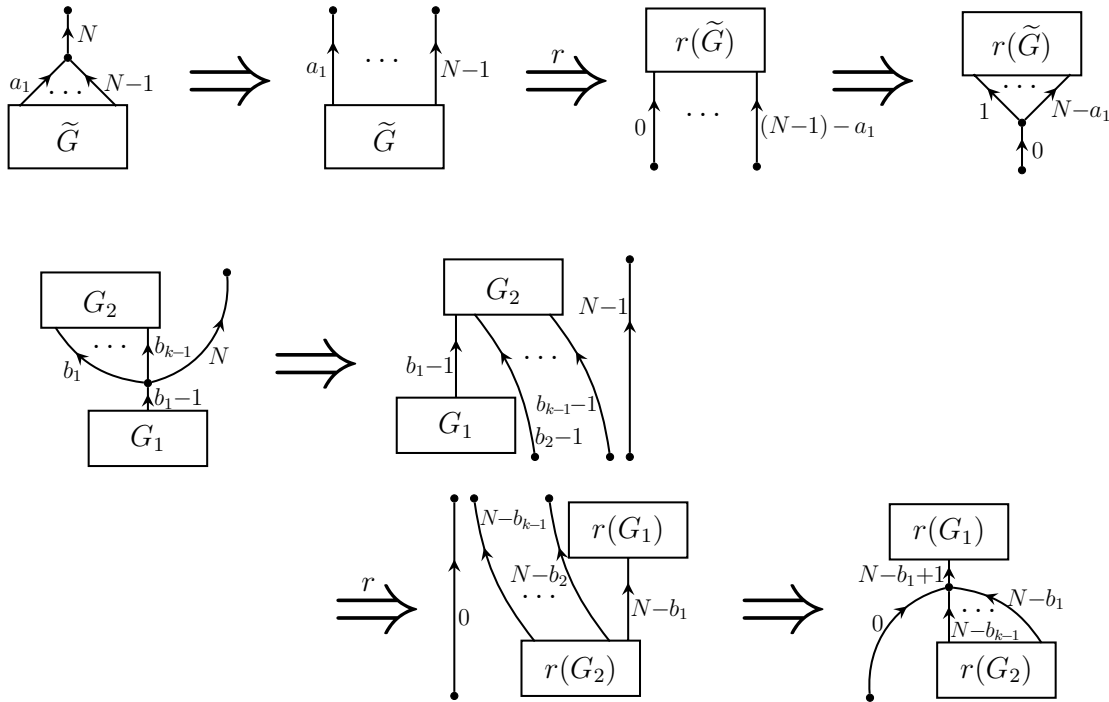


Figure 10: The effect of the rotation operator upon edge labels surrounding the final product node or coproduct node of $G \in \text{PC}_x^k(n, m)$, utilizing the “resolution” techniques from the proof of Proposition 4.4. In the top row, \tilde{G} may include additional output edges that lie to the left of the edge labelled N .

In the case of $x = 1$ and $n = m$, the rotation operator reduces to an involution $r : \text{PC}^k(n) \rightarrow \text{PC}^k(n)$ of closed k -ary prographs. Proposition 4.4 then states that the depth-left first search of Section 2 relates corresponding edges of G and $r(G)$ according to $i \mapsto (k + 1)n - i$. This allows us to derive the following relationship between the rotation operator on closed k -ary prographs, the Schützenberger involution on rectangular set-valued tableaux, and the bijection Φ from Theorem 2.1. See Figure 12 for an example of this compatibility.

Theorem 4.5. Fix $k \geq 2$ and $n \geq 1$, and let $\rho = (1, k - 1, 1)$. For $\Phi : \text{PC}^k(n) \rightarrow \mathbb{S}(\lambda, \rho)$ defined as in Theorem 2.1, the rotation operator $r : \text{PC}^k(n) \rightarrow \text{PC}^k(n)$, and the set-valued Schützenberger involution $f : \mathbb{S}(\lambda, \rho) \rightarrow \mathbb{S}(\lambda, \rho)$, we have $\Phi \circ r = f \circ \Phi$.

Proof. Take arbitrary $G \in \text{PC}^k(n)$ and set $N = (k + 1)n$, so that G contains $N + 1$ total edges and the cells of $\Phi(G) \in \mathbb{S}(\lambda, \rho)$ are filled with $\{1, \dots, N\}$. We show that leftmost coproduct children in G correspond to bottom row entries in both $\Phi \circ r(G)$ and $f \circ \Phi(G)$, while product outputs in G correspond to top row entries in both $\Phi \circ r(G)$ and $f \circ \Phi(G)$. This implies that $\Phi \circ r(G)$ and $f \circ \Phi(G)$ feature identical

sequences of integers across their top and bottom rows, and hence are the same tableau.

So assume G has been labelled according to our depth-left first search. By Proposition 4.4, if an edge in G is labelled with the integer a , then the corresponding edge in $r(G)$ is labelled with $N - a$. The depth-left first search is defined in such a way that a labels a leftmost coproduct output in G if and only if $a - 1$ labels the input to the same coproduct node for which a labels the leftmost child. As demonstrated in the left side of Figure 11, this means that $N - (a - 1)$ labels a product output in the rotated prograph $r(G)$. It follows that $N - a + 1$ appears in the bottom row of $\Phi \circ r(G)$. On the other hand, a being a leftmost coproduct child implies that a appears in the top row of $\Phi(G)$, and hence that $N - a + 1$ appears in the bottom row of $f \circ \Phi(G)$.

As r is an involution, the case where a labels a product in G follows directly from reversing the roles of G and $r(G)$ in the previous paragraph. See the right side of Figure 11 for a demonstration. In this case we may conclude that $N - a + 1$ appears in the top row of both $\Phi \circ r(G)$ and $f \circ \Phi(G)$, as required. \square

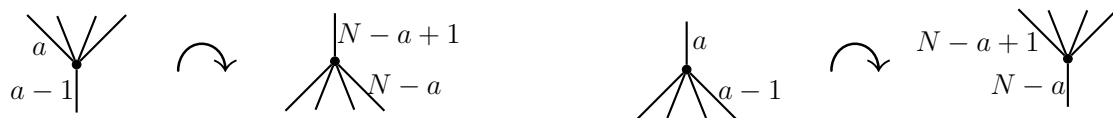


Figure 11: How the edge labels of leftmost coproduct outputs (left) and product outputs (right) behave under 180-degree rotation of the underlying prograph.

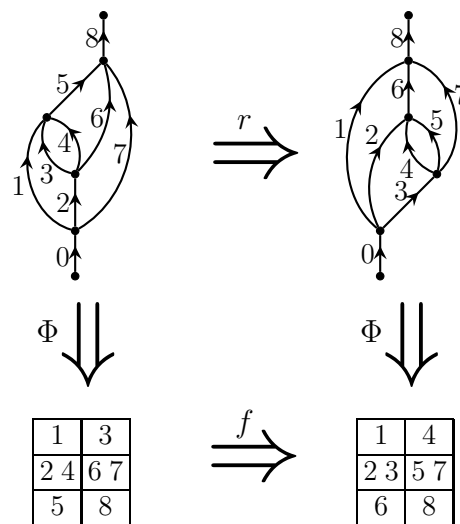


Figure 12: An example of the relationship between rotation r of k -ary product-coproduct prographs and the generalized Schützenberger involution f on standard set-valued Young tableaux.

As Proposition 4.4 applies to all x -fold k -ary prographs, the result of Theorem 4.5 may be directly extended to non-closed prographs if one defines a suitable generalization of the Schützenberger involution. If $\lambda = (n, n, n - a)$ and $\mu = (b, 0, 0)$, let $\lambda' = (n, n, n - b)$ and $\mu' = (a, 0, 0)$. Then there exists a map $F : \mathbb{S}(\lambda/\mu, \rho) \rightarrow \mathbb{S}(\lambda'/\mu', \rho)$ that is defined via 180-degree rotation of $T \in \mathbb{S}(\lambda/\mu, \rho)$ and a reversal $i \mapsto 3n - a - b + 1 - i$ of entries in the resulting tableau. This map clearly specializes to the Schützenberger involution when $a = b = 0$, and a superficial modification of the technique from Theorem 4.5 yields $\psi \circ r = F \circ \psi$. Notice how F flips the number of “missing boxes” in the top and bottom rows of a skew set-valued tableau, similarly to how r flips the number of “missing” products and coproducts needed to justify the associated x -fold prograph.

5 Future Directions

5.1 Non-Closed k -ary Prographs $\text{PC}_x^k(n, m)$ for which $x \not\equiv 1 \pmod{k-1}$

Subsection 4.1 entirely restricted its attention to sets $\text{PC}_x^k(n, m)$ of x -fold k -ary prographs for which $x \equiv 1 \pmod{k-1}$. Developing an analogue to Theorem 4.2 in the case of $x \not\equiv 1 \pmod{k-1}$ is significantly more involved, as such prographs require a modification of the justification operator whose effect on the associated set-valued tableaux is more difficult to interpret. Although we stop short of proving an explicit bijection, we pause to outline how the techniques of Subsection 4.1 may be generalized to the case of general $\text{PC}_x^k(n, m)$.

So let $x \equiv a \pmod{k-1}$, where $2 \leq a \leq k-1$, and consider the set $\text{PC}_x^k(n, m)$. There exists an injection $J : \text{PC}_x^k(n, m) \rightarrow \text{PC}^k(n + \frac{x+k-a-1}{k-1})$ in which $k-a$ free strands are added on the left side of $G \in \text{PC}_x^k(n, m)$, producing a prograph $\tilde{G} \in \text{PC}_{x+k-a}^k(n, m)$ in which the number of inputs is $1 \pmod{k-1}$, and then the original justification operator j is applied to \tilde{G} . For $G \in \text{PC}_x^k(n, m)$, we call the image $J(G) \in \text{PC}^k(n + \frac{x+k-a-1}{k-1})$ the **left-weighted justification** of G . See Figure 13 for an example of left-weighted justification.

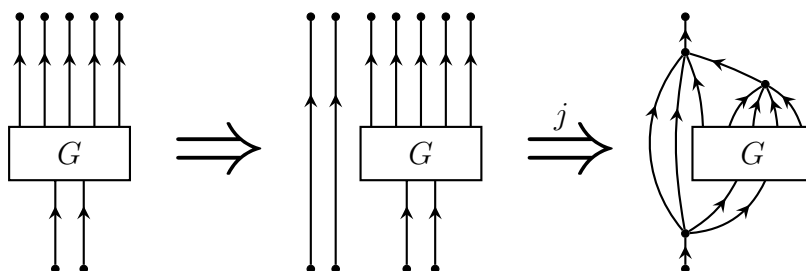


Figure 13: A non-closed prograph $G \in \text{PC}_2^4(n, n-1)$ and its left-weighted justification $J(G) \in \text{PC}^4(n + \frac{2+4-2-1}{4-1})$.

Following the techniques of Theorem 4.2, left-weighted justification suggests that $\text{PC}_x^k(n, m)$ may be placed in bijection with some subset of $\mathbb{S}(\lambda/\mu, \rho)$ for $\lambda = (n + \frac{x+k-a-1}{k-1}, n + \frac{x+k-a-1}{k-1}, m)$ and $\mu = (\frac{x+k-a-1}{k-1}, 0, 0)$. The difficulty is in describing what

subset of $\mathbb{S}(\lambda/\mu, \rho)$ corresponds to left-justified prographs in which the $k - a$ leftmost children of the initial coproduct terminate at the final product node.

Conjecture 5.1 describes the subset of $\mathbb{S}(\lambda/\mu, \rho)$ that should lie in bijection with $PC_x^k(n, m)$. The first condition below prevents the $k - a$ leftmost children of the initial coproduct from terminating at a coproduct node. The second condition prevents those same edges from serving as an input to a product that isn't the final product.

Conjecture 5.1. *Assume $x \equiv a \pmod{k - 1}$, where $2 \leq a \leq k - 1$. Then consider $PC_x^k(n, m)$ and $\mathbb{S}(\lambda/\mu, \rho)$ with $\lambda = (n + \frac{x+k-a-1}{k-1}, n + \frac{x+k-a-1}{k-1}, m)$ and $\mu = (\frac{x+k-a-1}{k-1}, 0, 0)$. For arbitrary $T \in \mathbb{S}(\lambda/\mu, \rho)$, let $b_1 < b_2 < \dots$ denote the middle-row entries of T and let $c_1 < c_2 < \dots$ denote the bottom-row entries of T . Then $PC_x^k(n, m)$ is in bijection with the subset of tableaux from $\mathbb{S}(\lambda/\mu, \rho)$ satisfying*

1. $b_i = i$ for all $1 \leq i \leq k - a$, and
2. $c_i > b_{(k-1)i+2-(k-a)}$ for all $1 \leq i \leq m - 1$.

5.2 Additional Combinatorial Interpretations

for $\mathbb{S}(n^3, \rho)$ with $\rho = (1, k - 1, 1)$

It is natural to suppose that all combinatorial interpretations of the three-dimensional Catalan numbers admit one-parameter generalizations that lie in bijection with the set $\mathbb{S}(n^3, \rho)$ for $\rho = (1, k - 1, 1)$. Below we briefly conjecture as to how several more of those interpretations may be k -generalized. See sequence A005789 of OEIS [12] for a full list of candidates. Beyond the interpretations discussed below, we are especially interested in how the pattern-avoiding permutations of Lewis [9] may be generalized using standard set-valued Young tableaux.

1. The three-dimensional Catalan number $C_{3,n}$ is known to count the number of walks in the first quadrant of \mathbb{Z}^2 that start and end at $(0, 0)$ and use $3n$ total steps from $\{(0, 1), (1, -1), (-1, 0)\}$. These walks are known to lie in bijection with $S(n^3)$ via a map that associates $(0, 1)$ steps with entries in the top row of the corresponding tableau, $(1, -1)$ steps with entries in the middle row of that tableau, and $(-1, 0)$ steps with entries in the bottom row of that tableau. We conjecture that this map may be generalized to a bijection between $\mathbb{S}(n^3, \rho)$ with $\rho = (1, k - 1, 1)$ and walks in the first quadrant of \mathbb{Z}^2 that start and end at $(0, 0)$ and which use $(k + 1)n$ total steps from $\{(0, k - 1), (1, -1), (-k + 1, 0)\}$. In this bijection, $(0, k - 1)$ steps should correspond to entries in the top row of the associated set-valued tableau, $(1, -1)$ steps should correspond to entries in the middle row of that tableau, and $(-k + 1, 0)$ steps should correspond to entries in the bottom row of that tableau.
2. $C_{3,n}$ is also known to count three-dimensional integer lattice paths from $(0, 0, 0)$ to (n, n, n) that use steps from $\{(1, 0, 0), (0, 1, 0), (0, 0, 1)\}$ and that satisfy $x \geq y \geq z$ at every lattice point (x, y, z) along the path. These lattice paths are known to lie in bijection with $S(n^3)$ via a map that associates $(1, 0, 0)$ steps

with entries in the top row of the corresponding tableau, $(0, 1, 0)$ steps with entries in the middle row of that tableau, and $(0, 0, 1)$ steps with entries in the bottom row of that tableau. It should be straightforward to generalize this map to a bijection between $\mathbb{S}(n^3, \rho)$ with $\rho(1, k - 1, 1)$ and integer lattice paths from $(0, 0, 0)$ to $((k - 1)n, n, (k - 1)n)$ that use steps from $\{(1, 0, 0), (0, 1, 0), (1, 0, 0)\}$ and which satisfy $(k - 1)x \geq y \geq (k - 1)z$ at every point (x, y, z) . This bijection would similarly associate $(1, 0, 0)$ steps to top-row entries, $(0, 1, 0)$ steps to middle-row entries, and $(0, 0, 1)$ steps to bottom-row entries.

For a somewhat different application of set-valued tableaux with $\rho = (1, k - 1, 1)$, we refer the reader to the work of Eu [5]. Eu places all standard Young tableaux with at most three rows and any shape $\lambda \vdash N$ in bijection with Motzkin paths of length n . By Motzkin paths of length n we mean integer lattice paths from $(0, 0)$ to $(n, 0)$ that use steps from $\{(1, 1), (1, -1), (1, 0)\}$ and never fall below the x -axis.

Direct computations for small n reveal that a similar result may hold for standard set-valued Young tableaux with at most three rows, precisely $n(k - 1)$ entries, and densities (determined by the number of rows) of either $\rho_1 = (1)$, $\rho_2 = (1, k - 1)$, or $\rho = (1, k - 1, 1)$. In particular, such tableaux appear to lie in bijection with what we refer to as $(k - 1)$ -sloped Motzkin paths of length n : lattice paths from $(0, 0)$ to $(n, 0)$ that use steps from $\{(k - 1, 1), (1, -1), (1, 0)\}$ and which never fall below the x -axis. The only caveat here is that one cannot include tableaux with “partially filled” cells: every cell must have the full complement of entries determined by ρ_i .¹

See Figure 14 for a comparison of 3-sloped Motzkin paths of length $n = 4$ and set-valued tableaux with density from $\{(1), (1, 2), (1, 2, 1)\}$ and precisely 4 entries. For justification of the specific matching exhibited in Figure 14, we direct the reader to the algorithm presented by Eu [5].

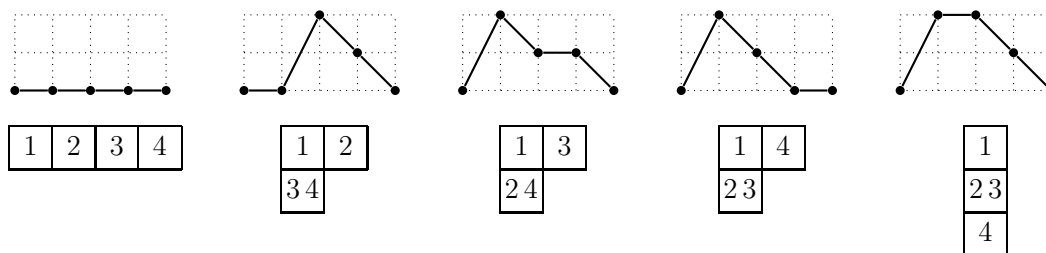


Figure 14: 3-sloped Motzkin paths of length 4 and standard set-valued Young tableaux with 4 entries across at most three-rows and densities of either $\rho_1 = (1)$, $\rho_2 = (1, 2)$, or $\rho_3 = (1, 2, 1)$.

5.3 $\mathbb{S}(\lambda, \rho)$ for Distinct Three- and Four-Row Densities

We close this paper by briefly exploring several additional densities for standard set-valued Young tableaux of shapes $\lambda = n^3$ and $\lambda = n^4$. The cardinalities of

¹ k -sloped Motzkin paths should not be confused with the pre-existing notion of k -Motzkin paths, which correspond to 2-sloped Motzkin paths in which every horizontal step carries one of k colors. See Barrucci, Del Lungo, Pergola and Pinazni [1] for a treatment of k -Motzkin paths

the resulting sets $\mathbb{S}(\lambda, \rho)$ correspond to one-parameter generalizations of the three- and four-dimensional Catalan numbers that are distinct from the three-dimensional k -Catalan numbers $C_{3,n}^k$ of previous sections. It is our hope that combinatorial interpretations as interesting as those for $C_{3,n}^k$ will eventually be found for each generalization.

First consider the case of $\lambda = n^3$ and $\tilde{\rho} = (k - 1, 1, 1)$, where $k \geq 1$. We informally refer to the resulting integers $\tilde{C}_{3,n}^k = |\mathbb{S}(n^3, \tilde{\rho})|$ as the non-involutory three-dimensional k -Catalan numbers. This title is motivated by the fact that the set-valued Schützenberger involution is no longer an automorphism of $\mathbb{S}(n^3, \tilde{\rho})$ but a bijection onto the distinct set $\mathbb{S}(n^3, \tilde{\rho}')$ with $\tilde{\rho}' = (1, 1, k - 1)$. Observe from Tables 1 and 2 of Appendix 5.3 that $\tilde{C}_{3,n}^k \leq C_{3,n}^k$ for all choices of n, k where both values are known.

Applying the methods of Section 3 to $\mathbb{S}(\lambda, \tilde{\rho})$ yields the closed formulas of Proposition 5.2 and the general recurrences of Proposition 5.3. See Table 2 of Appendix 5.3 for all known values of $\tilde{C}_{3,n}^k = |\mathbb{S}(n^3, \tilde{\rho})|$.

Pause to note that the recurrences of Proposition 5.3 are significantly harder to apply than those for $\rho = (1, k - 1, 1)$ that appear in Proposition 3.3, as the recurrences of Proposition 5.3 involve enumerations of (non-set-valued) standard skew Young tableaux. This is a difficulty that appears to extend to all three- (and four-) row densities other than $\rho = (1, k - 1, 1)$.

Proposition 5.2. *Let $\tilde{\rho} = (k - 1, 1, 1)$. For any $k \geq 1$,*

$$\tilde{C}_{3,2}^k = |\mathbb{S}(2^3, \tilde{\rho})| = \frac{1}{2}k^2 + \frac{3}{2}k,$$

$$\tilde{C}_{3,3}^k = |\mathbb{S}(3^3, \tilde{\rho})| = \frac{2}{3}k^4 + 3k^3 + \frac{7}{3}k^2 - k,$$

$$\tilde{C}_{3,4}^k = |\mathbb{S}(4^3, \tilde{\rho})| = \frac{25}{18}k^6 + \frac{61}{8}k^5 + \frac{175}{18}k^4 - \frac{35}{24}k^3 - \frac{37}{9}k^2 + \frac{5}{6}k.$$

Proposition 5.3. *Fix $k \geq 1$. For $\tilde{\rho} = (k - 1, 1, 1)$ and any three-row shape $\lambda = (a, b, c)$ with $a \leq b \leq c$,*

$$|\mathbb{S}((a, b, c), \tilde{\rho})| =$$

$$\begin{cases} \sum_{\substack{0 \leq j \leq i \leq b, \\ j \leq c}} \binom{b - i + c - j + k - 2}{k - 2} |S((b, c)/(i, j))| \cdot |\mathbb{S}((a - 1, i, j), \tilde{\rho})|, & \text{if } a > b; \\ \sum_{1 \leq i \leq c} |\mathbb{S}((a, b - 1, i), \tilde{\rho})|, & \text{if } a = b > c; \\ |\mathbb{S}((a, b, c - 1), \tilde{\rho})|, & \text{if } a = b = c. \end{cases}$$

In the case of $\lambda = n^4$, we recognize the densities $\xi_i = (1, k - 1, k - 1, 1)$ and $\xi_2 = (k - 1, 1, 1, 1)$ as prime candidates to obtain what should be referred to as

the (involution) four-dimensional k -Catalan numbers $C_{4,n}^k = |\mathbb{S}(4^n, \xi_1)|$ and the non-involution four-dimensional k -Catalan numbers $\tilde{C}_{4,n}^k = |\mathbb{S}(4^n, \xi_2)|$. As the addition of a fourth row makes the techniques of Section 3 significantly harder to apply, we simply direct the reader to Tables 3 and Table 4 of Appendix 5.3 for all known values of $C_{4,n}^k = |\mathbb{S}(4^n, \xi_1)|$ and $\tilde{C}_{4,n}^k = |\mathbb{S}(4^n, \xi_2)|$.

Acknowledgements

The authors would like to thank the Mathematics & Statistics Department of Valparaiso University, whose 2017 iteration of the VERUM REU (NSF Grant DMS-1559912) provided the framework under which this research took place. The authors would also like to thank Reviewer #1 for their many helpful comments and recommendations.

Appendix: Tables of Values

Values were obtained via a combination of proven results (Section 3, Subsection 5.3) and direct enumeration in Java. Java coding was performed by Benjamin Levandowski of Valparaiso University and is available upon request.

Table 1: Known values of $C_{3,n}^k = |\mathbb{S}(n^3, \rho)|$ for $\rho = (1, k - 1, 1)$.

$k \setminus n$	1	2	3	4	5	6
1	1	2	5	14	42	132
2	1	5	42	462	6006	87516
3	1	10	190	4295	153415	5396601
4	1	17	581	27461	1566018	100950800
5	1	26	1401	105026	9511451	
6	1	37	2890	315014	41500117	
7	1	50	5342	797917	144067106	

Table 2: Known values of $\tilde{C}_{3,n}^k = |\mathbb{S}(n^3, \tilde{\rho})|$ for $\tilde{\rho} = (k - 1, 1, 1)$.

$k \setminus n$	1	2	3	4	5	6
1	1	2	5	14	42	132
2	1	5	42	462	6006	87516
3	1	9	153	3579	101630	3288871
4	1	14	396	15830	779063	44072801
5	1	20	845	51325	3872370	
6	1	27	1590	136234	14589623	
7	1	35	2737	314202		

Table 3: Known values of $|\mathbb{S}(n^4, \xi_1)|$ for $\xi_1 = (1, k - 1, k - 1, 1)$.

$k \setminus n$	1	2	3	4	5	6
1	1	2	5	14	42	132
2	1	14	462	24024	1662804	140229804
3	1	84	24521	13074832		
4	1	460	960875	3959335892		
5	1	2380	31378194			
6	1	11814				
7	1	57288				

Table 4: Known values of $|\mathbb{S}(n^4, \xi_2)|$ for $\xi_2 = (k - 1, 1, 1, 1)$.

$k \setminus n$	1	2	3	4	5	6
1	1	5	42	462	6006	87516
2	1	14	462	24024	1662804	140229804
3	1	28	2158	281571	50972547	
4	1	48	6990	1798860	658138000	
5	1	75	18275	8103935		
6	1	110	41382	28950168		
7	1	154	84427			

References

- [1] E. Barrucci, A. Del Lungo, E. Pergola and R. Pinzani, A construction for enumerating k -coloured Motzkin paths, *Proc. First Annual Int. Conf. Computing and Combinatorics*, Springer (1995), 254–263.
- [2] N. Borie, Three-dimensional Catalan numbers and product-coproduct prographs, *Sém. Lothar. Combin.* **78B** (2017), Art. 39.
- [3] A. S. Buch, A Littlewood-Richardson rule for the K -theory of Grassmannians, *Acta. Math.* **189** (2002), #P2.4.
- [4] P. Drube, Set-valued tableaux and generalized Catalan numbers, *Australas. J. Combin.* **72**(1) (2018), 55–69.
- [5] S.-P. Eu, Skew-standard tableaux with three rows, *Adv. in Appl. Math.* **45**(4) (2010), 463–469.
- [6] J. Sutherland Frame, G. de B. Robinson and R. M. Thrall, The hook graphs of the symmetric group, *Canad. J. Math.* **6** (1954), no. 316, C324.
- [7] W. Fulton, *Young tableaux, with application to representation theory and geometry*, Cambridge University Press, 1996.
- [8] S. Heubach, N. Y. Li and T. Mansour, Staircase tilings and k -Catalan structures, *Discrete Math.* **308**(24) (2008), 5954–5964.

- [9] J. B. Lewis, Pattern avoidance for alternating permutations and Young tableaux, *J. Combin. Theory Ser. A* **118** (2011), 1436–1450.
- [10] C. Monical, Set-valued skyline fillings, *Sém. Lothar. Combin.* **78B** (2017), Art. 35.
- [11] V. Reiner, B. E. Tenner and A. Yong, Poset edge density, nearly reduced words, and barely set-valued tableaux. Preprint at arXiv:1603.09589 [math.CO] (2016).
- [12] OEIS Foundation Inc., The On-Line Encyclopedia of Integer Sequences, <http://oeis.org> (2018).

(Received 8 Oct 2017; revised 17 Feb 2018, 29 May 2018)